Automatic determination of robot tool centre point using a scalable network of photogrammetry sensors

Hao Xue[1], Oliver Martin[2], Nicholas Southon[2], Nan Yu[1]
[1]*School of Engineering, University of Edinburgh, EH9 3FB, UK*
[2]*Insphere Ltd, BS16 7FR, UK*

Abstract

This paper introduces a novel working prototype to automatically calibrate the tool centre point (TCP) of industrial robots using the IONA system, which is a scalable network of photogrammetric sensors. Today, the TCP is manually calibrated, however, this method is time-consuming and is highly reliant on skilled metrology operators. Poor calibration introduces a systemic error into the measurement, which reduces robot performance. Therefore, an automatic system for TCP calibration has been developed to solve this problem. The system consists of a portable TCP cube device, an artefact mounted on the robot end-effector and the IONA system. The calibration process uses the IONA system to quickly collect positional data (transformation & rotation) between the artefact on the end-effector and the reference sphere on the cube device. The frame of reference can be set to the artefact origin, and the transform to the reference sphere centre will be collected and analysed in the ORA software. The results are then fed to a least squares optimization algorithm, which can minimize the errors between the measured and fitted points using a sphere fitting model to get the best fitting sphere for determining the position of the TCP. The system functionality and accuracy will also be demonstrated.

1 Introduction

INSPHERE Ltd. is a company that specializes in utilizing metrology data to improve manufacturing processes, focusing on monitoring, and controlling industrial robotics. To improve the performance and increase potential applications of automation systems, INSPHERE has developed a measurement system: IONA. IONA is a photogrammetry-based system which detects the position of spherical retro-reflective targets within each camera (2D image space). A 3D position can be calculated with sub-millimetre accuracy by combining this data from multiple observations [1]. This paper discusses the use of the IONA system for automatic TCP calibration.

With the continuous development of intelligent manufacturing, industrial robots are becoming more widely used in different industries and challenging applications as they are a low-cost method for completing repetitive tasks [2]. One of the most significant characteristics of industrial robots is positional repeatability. Most serial-axis industrial robots today are typically highly repeatable (around 30-50μm) [1]. However, the accuracy of industrial robots is not always as good due to design limitations. For most industrial robots, the positioning accuracy is usually larger than 1 mm [3]. Unless than linear systems [4,5], even the smallest medical robot arms with the best precision can still make errors in positioning of more than 1 mm unless calibrated [6].

Commissioning errors, such as the definition of the transforms from robot flange to tool centre point (TCP), are a vital error source that affects the robot's accuracy. To overcome this error source and improve positional accuracy, a variety of TCP calibration methods - both manual and automatic - have been proposed.

For example, the most used traditional calibration tool in the manual method is the sharp-tipped tool [7]. Coordinate measurement machines (CMM) and laser trackers provide high-accuracy calibration results, but the costs are high [8]. As for automatic methods, image sensors and cameras can also be used for TCP calibration [9, 10]. Commercial equipment is also available for TCP calibration like the ABB Bullseye system is for arc welding tools and LEONI products are for different end effectors [11, 12].

Currently, INSPHERE calibrates the TCP position through a manual commissioning process, carried out by metrology experts using a laser tracker, which can provide a high calibration accuracy around 0.05 mm. However, this method is not always accurate and easy. The accuracy of this method highly relies on the skill of the operator, and it is also time-consuming to manually measure a TCP. TCP calibration is not a process that needs to be conducted only once during the installation phase [13]. Calibration may be needed after every wear and tip change. Therefore, an automatic calibration method is needed to resolve the existing difficulties and deskill the procedure.

2 Description of the Calibration System

The whole calibration system consists of an IONA system with four nodes mounted at four different corners around a FANUC robot arm, a verification artefact with a spike (representing a TCP tip) on the robot end-effector, a portable TCP cube device mounted on a tripod with reference sphere (calibration device) on it, and a Leica AT 960 laser tracker.

2.1 TCP Cube Device (Calibration Device)

The main part of the calibration system is the TCP cube device. A 6 mm ruby sphere is mounted on the top of the TCP cube as the reference sphere. Five tiles are used to form a cube shape device except for the bottom face of the cube, which is the base connected to a tripod. On each tile, four targets are positioned in a coded pattern, decoding defines a unique name for each of the targets. Each tile on both the TCP cube and verification artefact has a unique pattern of targets, which enables the IONA system to easily recognize these two different devices.

As shown in Figure 1 (a), four bars with a single target on the end are mounted on four different sides of the TCP cube to improve the calibration accuracy. In theory, tracking more targets in a more distributed manner will result in higher measuring accuracy. These external targets increase the measuring volume of the cube in space, and more targets will be tracked by the IONA system in a more distributed way. Therefore, the position of the reference sphere can be measured more accurately. However, during the real measuring process, these four single bars were not stable enough. The deflection of these bars resulted in lower measuring accuracy. Therefore, data from these extensions were not utilized for data analysis. The reason for adding only four single targets was to control the cost and make the system more practical. The cube shape of the calibration device is also easy for both manufacture and mounting.

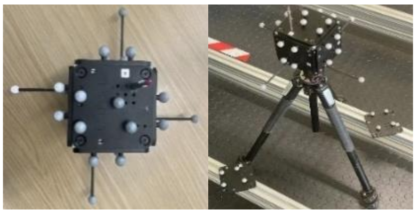

(a) (b)

Figure 1. TCP cube device: (a) TCP cube. (b) TCP cube on the tripod

2. 2 Verification Artefact with TCP Spike

A verification artefact was mounted on the robot end-effector to represent a real tool. The verification artefact is a large cube shape device, with a Leica T-Mac (Tracker-Machine control sensor) mounted on the front face. T-Mac is a 6 DoF (Degree of freedom) tracking device for automated applications [14]. With the T-Mac and the laser tracker, visual feedback for process information can be checked on the computer for later accuracy verification of the IONA system. On each face of the artefact except the front and back faces, two groups of targets are mounted for being identified by IONA system.

As Figure 2(a) and 2(c) show, a spike was mounted on the bottom face of the artefact as a TCP tip, and the TCP position is defined at the tip of this spike. After the measuring process, the real TCP position would be measured manually using a Leica AT 960 laser tracker and compared to the calculated results using the automated algorithm to validate the accuracy of the automated method.

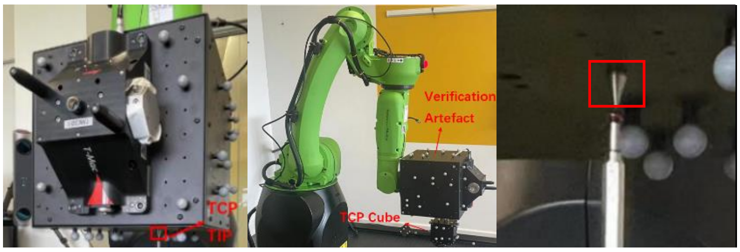

(a) (b) (c)

Figure 2. Verification artefact: (a) Verification with TCP tip. (b)Verification artefact with TCP cube device. (c) TCP tip

2.3 Nodes

Four IONA nodes were mounted at four different corners around the FANUC robot arm. These four nodes formed a network that can measure the entire system in a complete view without blind angle, which increased measuring accuracy.

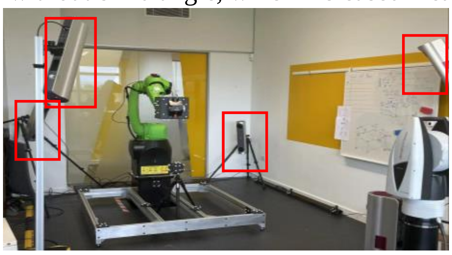

Figure 3. Four nodes around the FANUC robot arm (system overview)

3 Measurement Procedure

The idea of the prototype system is based on the traditional TCP calibration method: collecting and analysing data by a series of measurements done at different orientations of the robot probing a fixed reference sphere [7].

In our design, there will be nine probing directions for the TCP tip as Figure 4 (a). However, direction three is impossible to reach with the robot arm. Therefore, only eight directions except direction three are chosen for measuring (note: direction one is from the top of the reference sphere). In addition, the TCP cube can be moved to make the probing of the tip easier since the cube is also tracked by the IONA system.

The ORA software is specially designed for the IONA system, which can record frames three times every second. The IONA system will be used for measuring for around 15 seconds at every TCP tip position. Therefore, around 45 frames will be recorded at every position.

In addition, as Figure 4 (b), two different measuring positions of the TCP cube device are chosen to check whether distinct positions of the reference sphere will affect the accuracy of the IONA system. The second position is further from the centre of the measurement volume than the first one.

The whole procedure is summarized as follows:

1). Set the TCP cube device stably on the base and use the laser tracker to calibrate all the targets on the cube device and the verification artefact for the measurement of the IONA system.

2). Attach the cube device to a tripod and place it in the first position for measuring (The height of the cube should be higher than the base of the robot). Jog the TCP tip to probe the reference sphere and collect positional data from eight different directions using the ORA software. All the positional data like x, y, z, Rx, Ry, and Rz (a 'frame' in the ORA software) will be recorded.

3). Place the tripod in the second position for measuring. The whole process is the same as at position one.

4). After the testing in position two, place the cube device back to position one and repeat steps two and three for two times as a repeatability test to validate the accuracy and reliability of this method.

5). Use a laser tracker (Leica AT960 & T-Probe) to manually measure the TCP position. Compare the laser tracker's results with IONA's results to validate the accuracy and efficiency of the IONA system.

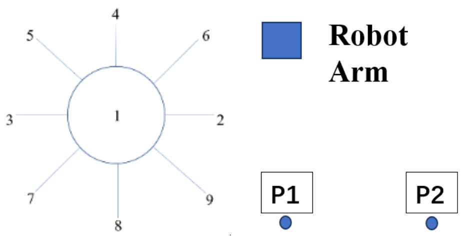

(a) (b)

Figure 4. Diagram of the measurement procedure: (a) TCP tip direction configuration. (b) Configuration of two TCP cube device positions

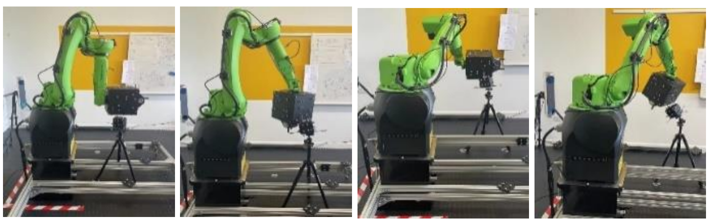

(a) (b) (c) (d)

Figure 5. Different repeatability tests in position one and two: (a) Position one direction one (b) Position one direction eight (c) Position two direction four (d) Position two direction eight

4 Algorithm and Data Analysis

4.1 Least Squares Sphere Fitting

The positional data collected by the IONA system is a three-dimensional data set suited for sphere fitting. To use the least squares method, the equation of a sphere needs to be first rearranged. Using the rearranged form of the equation, the sphere can be fitted to a set of three-dimensional data points more intuitively.

The general equation of a sphere in x, y and z coordinates is as following:

$$(x - x_0)^2 + (y - y_0)^2 + (z - z_0)^2 = r^2 \tag{1}$$

where the centre point of the sphere is (x_0, y_0, z_0).

After expanding and rearranging the original equation, the new equation of the sphere can be shown as:

$$x^2 + y^2 + z^2 = 2xx_0 + 2yy_0 + 2zz_0 + r^2 - {x_0}^2 - {y_0}^2 - {z_0}^2 \tag{2}$$

Then, this equation form can be expressed in vector/matrix form to generate a new equation.

$$\vec{f} = A\vec{c} \tag{3}$$

The $\vec{f}$, $\vec{c}$ vector and A matrix represent the consolidated terms of the expanded equation.

$$\vec{f} = \begin{bmatrix} x_i^2 + y_i^2 + z_i^2 \\ x_{i+1}^2 + y_{i+1}^2 + z_{i+1}^2 \\ \vdots \\ x_n^2 + y_n^2 + z_n^2 \end{bmatrix} \tag{4}$$

$$A = \begin{bmatrix} 2x_i & 2y_i & 2z_i & 1 \\ 2x_{i+1} & 2y_{i+1} & 2z_{i+1} & 1 \\ \vdots & \vdots & \vdots & \vdots \\ 2x_n & 2y_n & 2z_n & 1 \end{bmatrix} \tag{5}$$

$$\vec{c} = \begin{bmatrix} x_0 \\ y_0 \\ z_0 \\ r^2 - {x_0}^2 - {y_0}^2 - {z_0}^2 \end{bmatrix} \tag{6}$$

The items x_i, y_i and z_i represent the first data point on the sphere, while x_n, y_n and z_n represent the last data point. The least-square sphere fitting method will determine the best $\vec{c}$ using the collected data points. The radius of the sphere can then be calculated using the terms in $\vec{c}$.

The above equation can be used to define a Python function that will fit a sphere to x, y, and z data points. The Python SciPy library includes a least squares function used to determine the best $\vec{c}$. The radius and centre coordinates of the sphere can also be returned by this function [15].

4.2 Data Analysis

During the test, two opposite directions were recorded for every frame, the first direction is from the ruby sphere centre to the constellation origin of the verification artefact. The other direction is the opposite. These two kinds of frames resulted in two different methods for analysing the TCP position.

To simplify modelling and analysis, the TCP tip radius is ignored in the coding process.

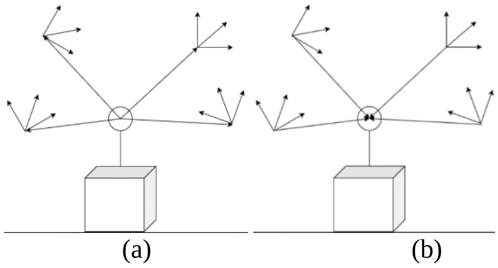

Figure 6. Two transform directions: (a) Cube Sphere Centre -> Verification Artefact Origin. (b) Verification Artefact. Origin -> Cube Sphere Centre

Method 1

The first method uses the transform from the ruby sphere centre to the origin of the verification artefact as Figure 6(a) shows. In this situation, the position of the ruby sphere centre in the overall coordinate system is nominal: (0, 0, 0).

Different coordinate frames in this figure represent distinct positions of the verification artefact origin at different TCP tip direction.

Using the collected data, a large sphere around the ruby sphere centre can be fitted as Figure 7.

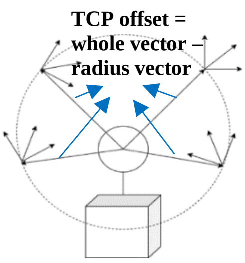

Figure 7. Method one sphere fitting

Using the least squares method mentioned above, the radius of this best-fitted sphere can be calculated. For every measured frame, the contact point of the ruby sphere with the transform from the ruby sphere centre to the artefact frame is the TCP position (tip of the spike) at that moment.

INSPHERE is interested in establishing the transformation between constellation origin to the TCP. In other words, the corresponding estimation of the TCP offset can be calculated using the vector form of collected path minus the radius vector (normalized path vector multiplying by the ruby sphere radius). The TCP's x, y, and z coordinates can then be resolved for each measured frame. After this calculation, the average of every TCP's x, y, and z coordinates can be obtained as the final TCP position from constellation origin.

Method 2

The second method uses the path from the origin of the verification artefact to the ruby sphere centre, as Figure 6(b) shows. This method is similar to the traditional manual method based on touching a fixed reference sphere. The collected data forms a small sphere around the ruby sphere. The estimated TCP position is the contact point of this sphere and the path. The centre of the fitted sphere has the same x and y coordinates as the TCP. However, there is an offset in z direction between the sphere centre and the TCP since the TCP is on the fitted sphere surface. The length of this offset should be the same as the radius of the ruby sphere, which is 3 mm. Therefore, the z coordinate of the TCP should be the z coordinate of the fitted sphere centre plus 3 mm.

5 Validation and Results

During the test, the path was recorded as $p_i = \left(x_i, y_i, z_i, R_{x_i}, R_{y_i} R_{z_i}\right), i = 1, \ldots, n$, where i is the measuring time. For eight directions of the tip, eight different kinds of paths were generated. Using this data as the input of the algorithm, the number of collected points, x, y, and z coordinates of the fitted sphere centre and the radius of the fitted sphere can be obtained. Then the x, y, and z coordinates of the TCP position can be inferred.

For method one, an averaging method is used to achieve higher accuracy: generating the TCP position using every path and averaging all the TCP positions as the result. For method two, all paths are used for the sphere fitting.

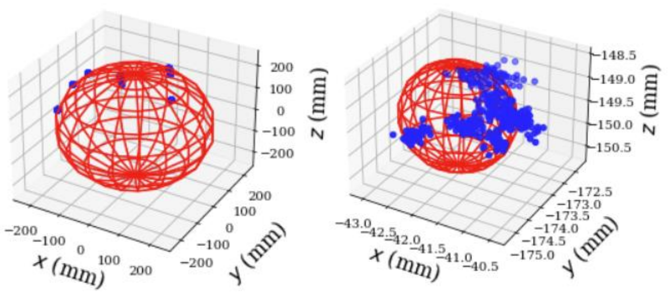

(a) (b)

Figure 8. Fitted sphere: (a) Fitted sphere -position one repeat test one (method one). (b) Fitted sphere -position one repeat test one (method two)

As Figure 8 shows, the fitted sphere radii in each method are orders of magnitude different. In method one, a much larger sphere is fitted compared to method two.

The TCP position measured by the manual method is:

[-41.612,-174.279,-145.913]

The errors in Table 1 are calculated by subtracting the manually measured TCP position from all estimated TCP positions.

Table 1. Errors of method one and two compared to the manual method [mm]

	Error x Method 1	Error x Method 2	Error y Method 1	Error y Method 2	Error z Method 1	Error z Method 2
Position 1 Repeat 1	0.55	-0.42	2.64	0.59	-1.49	-0.70
Position 1 Repeat 2	0.23	-0.09	2.06	-0.64	-1.64	-0.21
Position 1 Repeat 3	1.02	0.73	1.81	-0.46	-1.40	-0.63
Position 2 Repeat 1	0.24	-0.27	1.72	-0.77	-1.64	-1.13
Position 2 Repeat 2	0.35	-0.64	1.76	-0.33	-1.70	-0.83
Position 2 Repeat 3	0.87	0.66	2.01	0.14	-1.53	-0.25
Position 1 average	0.60	0.08	2.17	-0.17	-1.51	-0.51
Position 2 average	0.48	-0.08	1.83	-0.32	-1.62	-0.74

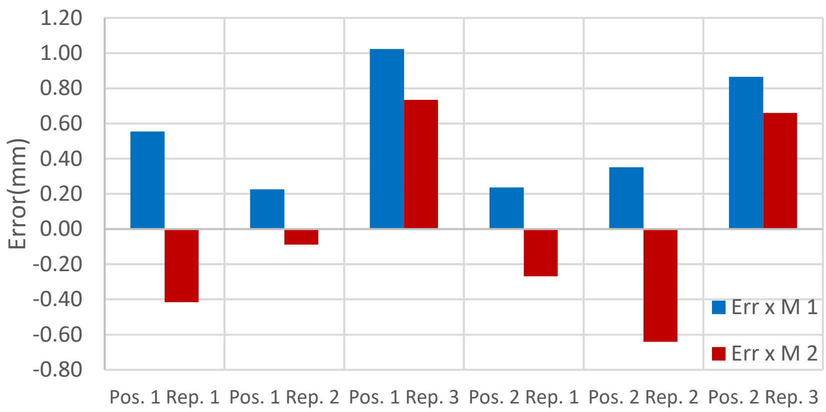

Figure 9. Errors of x-axis of two methods

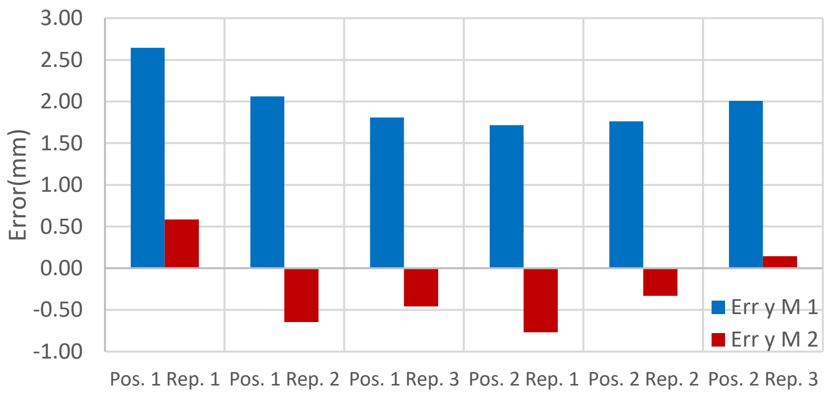

Figure 10. Errors of y-axis of two methods

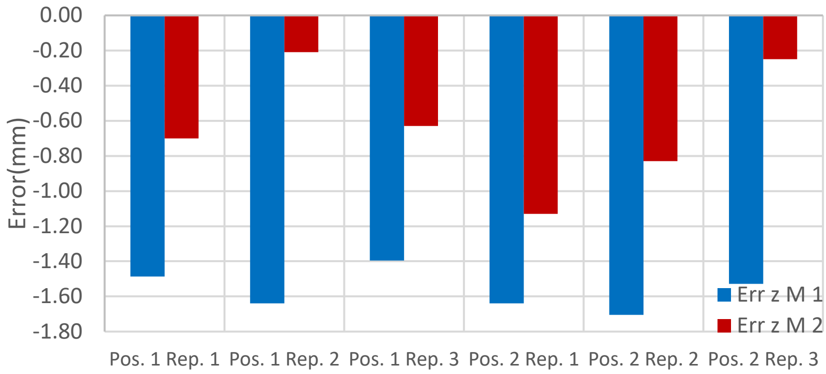

Figure 11. Errors of z-axis of two methods

Table 1, Figure 9, 10 and 11, respectively, show errors in the x-, y- and z-axis of these two methods. By comparing the errors of method one and two, it is obvious that method two has higher accuracy in all directions.

For method two, the accuracy is close to the manual laser tracker method. In both the x- and y-axis, all the errors are controlled within the range $\pm$ 0.8 mm. The average errors in the x-axis in position one and position two are only 0.08 mm and -0.08 mm, which proves the high accuracy of the automated method. In the y-axis, the average errors are -0.17 mm and -0.32 mm, which are still accurate. In the z-axis, most errors are controlled within -1 mm and the average errors are -0.51 mm and -0.74 mm in two different positions. The accuracy in the z-axis is acceptable for a first-edition prototype but still needs to be improved in future developments. For example, developing a new data collecting method and a data cleaning method to reduce the effect of the noises in the dataset.

6 Conclusion

This paper has proposed a novel automated method for accurately calibrating the TCP of an industrial robot using an IONA system. Compared to the current manual laser tracker method, this automated method is simpler and more efficient even for operators without professional metrology skills.

It was found that the accuracy of this new method is close to that of a laser tracker. However, the calibration time was saved. This new method takes around 15-20 minutes while the manual method takes an efficient operator around half an hour. In addition, operator experience is reduced for this method.

To improve the accuracy of metrology, more research is needed. For example, develop a new data-collecting method to increase the coverage percentage of the collected data on the fitted sphere. In addition, developing a data cleaning method which can automatically remove the noises and outliers will be helpful. The improvement of test devices like increasing the stiffness of the bars on the TCP cube is also another important development direction.

References

[1] Martin, O. (2022). Confronting the Challenges Associated with Measuring Industrial Robots. Proceeding of the CMSC conference, 2022

[2] Gasparetto, A. and Scalera, L. (2019). A Brief History of Industrial Robotics in the 20th Century. Advances in Historical Studies, 08(01), 24–35. doi:10.4236/ahs.2019.81002.

[3] Muelaner, J.E., Wang, Z. and Maropoulos, P.G. (2011). Concepts for and analysis of a high accuracy and high capacity (HAHC) aerospace robot. Proceedings of the Institution of Mechanical Engineers, Part B: Journal of Engineering Manufacture, 225(8), 1393–1399.

[4]. Matsukuma, H., Adachi, K., Sugawara, T., Shimizu, Y., Gao, W., Niwa, E., & Sasaki, Y. (2021). Closed-Loop Control of an XYZ Micro-Stage and Designing of Mechanical Structure for Reduction in Motion Errors. Nanomanufacturing and Metrology, 4, 53-66.

[5] Ohashi, T., Shibata, H., Futami, S., & Sato, R. (2021). Nanometer-order contouring control in a feed drive system using linear ball guides by applying a combination of modified disturbance observer and repetitive control. Nanomanufacturing and Metrology, 4, 118-129.

[6] Icli, C., Stepanenko, O., & Bonev, I. (2020). New method and portable measurement device for the calibration of industrial robots. Sensors (Switzerland), 20(20), 1–15.

[7] Zhang, L., Li, C., Fan, Y., Zhang, X. and Zhao, J. (2021). Physician-Friendly Tool Center Point Calibration Method for Robot-Assisted Puncture Surgery. Sensors, 21(2), p.366. doi:10.3390/s21020366.

[8] Cakir, M. and Deniz, C. (2019). High precise and zero-cost solution for fully automatic industrial robot TCP calibration. Industrial Robot: the international journal of robotics research and application, 46(5), 650–659. doi:10.1108/ir-03-2019-0040.

[9] Luo, R.C. and Wang, H. (2018). Automated Tool Coordinate Calibration System of an Industrial Robot. 2018 IEEE/RSJ International Conference on Intelligent Robots and Systems (IROS). doi:10.1109/iros.2018.8594298.

[10] Gordic, Z. and Ongaro, C. (2016). Calibration of robot tool centre point using camera-based system. Serbian Journal of Electrical Engineering, 13(1), 9–20. doi:10.2298/sjee1601009g.

[11] Henry F. Throne, Pittsburgh, Pa. (1995), Tool centre point calibration apparatus and method. United States Patent, Patent Number: 5457367.

[12] Zwierzchowski, J. (2017). A Device For Automatic Robot Tool Centre Point (TCP) Calibration Adjustment For The Abb Industrial Robots. 15–18.

[13] Sun, Y., Giblin, D.J. and Kazerounian, K. (2009). Accurate robotic belt grinding of workpieces with complex geometries using relative calibration techniques. Robotics and Computer-Integrated Manufacturing, 25(1), 204–210. doi:10.1016/j.rcim.2007.11.005.

[14] Hexagon Manufacturing Intelligence. Leica T-Mac. [online] Available at: https://www.hexagonmi.com/products/laser-tracker-systems/leica-tmac.

[15] Charles Jekel - jekel.me - Least Squares Sphere Fit. [online] Available at: https://jekel.me/2015/Least-Squares-Sphere-Fit/ .